Atmos. Chem. Phys. Discuss., 11, 7095–7112, 2011
www.atmos-chem-phys-discuss.net/11/7095/2011/
doi:10.5194/acpd-11-7095-2011

Atmospheric Chemistry and Physics Discussions

Changes in organic aerosol composition with aging inferred from aerosol mass spectra

N. L. Ng[1], M. R. Canagaratna[1], J. L. Jimenez[2,3], P. S. Chhabra[4], J. H. Seinfeld[4], and D. R. Worsnop[1]

[1]Aerodyne Research, Inc. Billerica, MA, USA
[2]Department of Chemistry and Biochemistry, University of Colorado, Boulder, CO, USA
[3]CIRES, University of Colorado, Boulder, CO, USA
[4]Department of Chemical Engineering, California Institute of Technology, Pasadena, CA, USA

Received: 23 February 2011 – Accepted: 23 February 2011 – Published: 2 March 2011

Correspondence to: M. R. Canagaratna (mrcana@aerodyne.com)

Published by Copernicus Publications on behalf of the European Geosciences Union.

Abstract

Organic aerosols (OA) can be separated with factor analysis of aerosol mass spectrometer (AMS) data into hydrocarbon-like OA (HOA) and oxygenated OA (OOA). We develop a new method to parameterize H:C of OOA in terms of f_{43} (ratio of m/z 43, mostly $C_2H_3O^+$, to total signal in the component mass spectrum). Such parameterization allows the transformation of large database of ambient OOA components from the f_{44} (mostly CO_2^+, likely from acid groups) vs. f_{43} space ("triangle plot") (Ng et al., 2010) into the Van Krevelen diagram (H:C vs. O:C). Heald et al. (2010) suggested that the bulk composition of OA line up in the Van Krevelen diagram with a slope ~ -1; such slope can potentially arise from the physical mixing of HOA and OOA, and/or from chemical aging of these components. In this study, we find that the OOA components from all sites occupy an area in the Van Krevelen space, with the evolution of OOA following a shallower slope of ~ -0.5, consistent with the additions of both acid *and* alcohol functional groups without fragmentation, and/or the addition of acid groups with C-C bond breakage. The importance of acid formation in OOA evolution is consistent with increasing f_{44} in the triangle plot with photochemical age. These results provide a framework for linking the bulk aerosol chemical composition evolution to molecular-level studies.

1 Introduction

The study of organic aerosols (OA) in the atmosphere is challenging due to the large number of molecular species involved and the continuous evolution of OA concentration, composition, and properties (Jimenez et al., 2009). Recently, simplified ways of characterizing the aging of OA in the atmosphere from aerosol mass spectrometer (AMS) datasets have been identified (Ng et al., 2010; Heald et al., 2010). Ng et al. (2010) analyzed OA components determined from positive matrix factorization (PMF) analysis of 43 AMS datasets in the Northern Hemisphere (unit mass

ACPD
11, 7095–7112, 2011

resolution mass spectra, UMR, and high resolution, HR). At most sites, OA could be separated into hydrocarbon-like OA (HOA) and oxygenated OA (OOA), and sometimes other primary components. OOA is a good surrogate for SOA under most conditions (Jimenez et al., 2009) and can be further deconvolved into semi-volatile OOA (SV-OOA) and low-volatility OOA (LV-OOA). OA evolution is characterized in terms of the changing intensities of the two most dominant oxygen-containing ions in the OOA spectra, *m/z* 44 (mostly CO_2^+ in ambient data) and *m/z* 43 (mostly $C_2H_3O^+$). The ion *m/z* 44 is thought to be due mostly to acids (Duplissy et al., 2011) or acid-derived species, such as esters. The *m/z* 43 ion is predominantly due to non-acid oxygenates. Both acid and non-acid oxygenates have been observed in ambient OA (Russell et al., 2011; Decesari et al., 2007). When f_{44} (ratio of *m/z* 44 to total signal in the component spectrum) is plotted against f_{43} (defined similarly), all OA components fall within a triangular space (Fig. 1, hereafter referred to as the "triangle plot"). The HOA components have $f_{44} < 0.05$; SV-OOA and LV-OOA components concentrate in the lower and upper halves of the triangle, respectively. The *m/z* 43 fragment is mainly $C_2H_3O^+$ for the OOA components, and $C_3H_7^+$ for the HOA components. The base of the triangle encompasses the variability in HOA and SV-OOA composition. This range decreases with increasing f_{44} (O:C ratio), suggesting that the aerosols become more chemically similar with increasing aging, largely independent of the initial source of the material (Jimenez et al., 2009; Ng et al., 2010). Most SOA produced in the laboratory cluster on the lower half of the triangle, indicating that they are not as oxidized as ambient LV-OOA (Ng et al., 2010).

Heald et al. (2010) characterized the evolution of bulk OA composition using the Van Krevelen diagram (H:C vs. O:C) (Van Krevelen, 1950). In this approach, high resolution mass spectra were analyzed to obtain bulk H:C and O:C values (Aiken et al., 2007; Aiken et al., 2008). HR-AMS field datasets and laboratory studies occupy a narrow range when plotted in the Van Krevelen diagram. The authors reported that all the data cluster along a line with slope ~ -1, consistent with simultaneous increases in carbonyl and alcohol moieties, either in separate carbons or due to the addition of

ACPD
11, 7095–7112, 2011

carboxylic acid groups. It is suggested that the aerosol composition moves along this line with increased aging (Heald et al., 2010).

In this work, we link the complementary information of the triangle plot and the Van Krevelen diagram to provide further understanding of atmospheric OA evolution. The triangle plot provides an empirical way of viewing all new AMS data in the context of available data for characterizing aerosol aging; data obtained from both UMR (such as the Q-AMS and the recently developed Aerosol Chemical Speciation Monitor, ACSM, (Ng et al., 2011)) and HR instruments can be readily plotted in real time in this space. With detailed data processing of HR-AMS data, the added chemical insight contained in the Van Krevelen diagram provides information on the mechanism of evolution of OA composition.

1.1 Methods: parameterization of H:C vs. f_{43}

In order to map data from the triangle plot (f_{44} vs. f_{43}) onto the Van Krevelen diagram (H:C vs. O:C), both H:C and O:C must be parameterized using UMR data. Aiken et al. (2008) showed that O:C of ambient OA can be estimated from f_{44} through a linear parameterization. In this work, we obtain an analogous parameterization of H:C in terms of f_{43} (Fig. 2) for SOA/OOA, using OOA components obtained from PMF analysis of HR-AMS ambient datasets (Docherty et al., 2008; Aiken et al., 2009; DeCarlo et al., 2010; Huang et al., 2010a, b; Sun et al., 2011) and SOA formed in laboratory studies (Chhabra et al., 2010; 2011, Massoli et al., 2010). All the data shown are HR, in which H:C is determined explicitly by elemental analysis. As these are OOA/SOA data, f_{43} in Fig. 2 is dominated by the oxygenated fragment at m/z 43, i.e., $C_2H_3O^+$. The laboratory studies include both chamber (Chhabra et al., 2010, 2011) and flow tube experiments (Massoli et al., 2010), encompassing a wide range of precursors (anthropogenic and biogenic) and degree of oxidation (hours to ~2 weeks of photooxidation). The data are fitted to a polynomial function. The y-intercept is constrained to an H:C of 1.0, which corresponds to aromatic SOA precursors which often have the lowest H:C values. We caution that this parameterization is only valid for

ACPD
11, 7095–7112, 2011

$0.05 < f_{43}$ ($C_2H_3O^+$) < 0.25 and $f_{44} > 0.06$ (Fig. S1). These ranges overlap well with all the ambient OOA components in the triangle plot (Fig. 1). It appears that the HOA and other OA components (local OA (LOA), biomass burning OA (BBOA), cooking OA (COA)) where $C_3H_7^+$ contributes $>\sim 20\%$ of *m/z* 43 may require a separate parameterization (Fig. S2) and warrants future investigation.

2 Results and discussion

2.1 Field measurements

The OOA components in the triangle plot are transformed into the Van Krevelen diagram using the parameterization, and the results are shown in Fig. 3. The left and right sides of the triangle plot become the bottom and top lines in the Van Krevelen diagram, respectively. The light green points are SV-OOA which has lower O:C, while the dark green data are LV-OOA which has higher O:C. We refer to Fig. 3 as the "VK-triangle" diagram. Histograms showing the distribution of the estimated H:C ratios and the carbon oxidation states ($\overline{OS}_C \approx 2$ O/C – H/C) (Kroll et al., 2011) observed across multiple sites are shown in Fig. 4b and c, respectively. Carbon oxidation state is found to be a useful metric for describing the chemistry of atmospheric organic aerosol (Kroll et al., 2011). The variation in f_{43} of the SV-OOA components in the triangle plot is still preserved in the VK-triangle diagram, with SV-OOA components spanning a range of H:C ratios. Possible reasons for the range of observed H:C ratios include the different SOA precursor mixes and chemical pathways of SOA formation. For instance, the chamber data from photooxidation of methyl chavicol ($C_{10}H_{12}O$) and linalool ($C_{10}H_{18}O$) span the base of the triangle plot (Fig. 1); these data roughly define the intercepts of the two lines that made up the VK-triangle, which is consistent with the H:C ratios of the precursor hydrocarbon (i.e. H:C = 1.2 for methyl chavicol, H:C = 1.8 for linalool).

ACPD
11, 7095–7112, 2011

There are two observations from this VK-triangle diagram that differ from those in Heald et al. (2010): (1) Most data points in Heald et al. (2010) cluster around the line with the −1 slope, with only some points at high O:C showing a lower slope of ∼ −0.8. In Fig. 3, however, the data points span a larger region in the diagram; (2) on average, the transition from SV-OOA to LV-OOA follows a line with a slope that is shallower than −1 (∼ −0.5). Only four HR OOA components were available at the time of Heald et al. (2010), which may explain why these features are not clear in that study.

Other than Mexico City (flight and ground) (Aiken et al., 2009; DeCarlo et al., 2010), the OA components from other HR datasets (Riverside, Queens NY, China PRD, Beijing) (Docherty et al., 2008, Sun et al., 2011; Huang et al., 2010a, 2010b) have also become available recently. The OA components from all these sites and the results from the heterogeneous oxidation of squalane (Kroll et al., 2009) are shown in Fig. 5. The OOA components from these HR datasets mostly fall into the VK-triangle region defined by the UMR data while the HOA components and the squalane data are outside the VK-triangle region. As most data in Heald et al. (2010) represent the average OA composition at each site, the observed slope of ∼ −1 in their study can arise from a combination of physical mixing of HOA and OOA components, and/or chemical evolution of these components. The HOA, SV-OOA, and LV-OOA components from Riverside are highlighted in Fig. 5. It is clear that once the total OA is deconvolved into these components, the evolution of SV-OOA to LV-OOA follows a shallower slope. The differences in primary OA components (HOA, LOA, BBOA, COA) likely reflect some atmospheric evolution, but are not easily interpreted since they also likely represent differences in the initially emitted POA. However, the squalane data suggest that the initial heterogeneous oxidation of POA species may follow a steeper slope, consistent with carbonyl group addition. This corresponds to the horizontal movement of the squalane data across the triangle plot (Fig. 1), with larger increase in f_{43} due to non-acid oxygenates (such as carbonyls) and relatively smaller increase in f_{44} (acids). Freshly formed SOA, represented by SV-OOA, evolves in a different way, with a shallower slope of ∼ −0.5. It is possible that further aging of oxidized HOA which has

ACPD
11, 7095–7112, 2011

reached the SV-OOA region of the VK-triangle may also proceed with the shallower slope, as hinted by the change in slope of the evolution of squalane oxidation products in Fig. 5. However, this is not definitive from the available ambient data.

A slope of ∼ −0.5 in the Van Krevelen diagram can be explained by at least two systematic OA chemical transformations mechanisms. If the functional group addition occurs on a CH_2 group without C-C bond breakage, this slope can be caused by e.g., the addition of 3 OH groups and 1 C = O group, or the addition of 2 OH groups and 1 COOH group. A movement to the right (increase in O:C) with the gentler slope (∼ −0.5) in the Van Krevelen diagram is equivalent to a movement up the triangle plot (increase in f_{44}). Since *m/z* 44 is found to be proportional to the acid content of standard compounds (Duplissy et al., 2011), it is likely that acid group formation plays an important role in the aging of SOA. Therefore, an OOA aging mechanism that is consistent with measurements (laboratory + field data) is that the ensemble average of the transformation involves both the net addition of COOH *and* OH functional groups. An alternative explanation for a slope of −0.5 is due to COOH group addition to the site of a C-C bond cleavage. For instance, the replacement of a $-CH_2$ group with a −COOH group at a C-C bond breakage (without loss of oxygen during the fragmentation process) will result in a slope of −0.5 in the Van Krevelen diagram. Fragmentation is thought to become increasingly important for already oxidized material such as fresh SOA (Kroll et al., 2009, 2011).

2.2 Laboratory data

Photooxidation of α-pinene provides a laboratory case study to illustrate aerosol composition changes in the VK-triangle space for a simpler, globally important, and well-studied SOA system (Fig. 6). The data shown in Fig. 6 includes HR-AMS data from both chamber and flow tube experiments (Chhabra et al., 2010, 2011; Massoli et al., 2010). In the chamber experiments, typical atmospheric OH levels are employed for hours, resulting in moderate oxidation, i.e. O:C ∼ 0.3 in the SV-OOA range. OH exposures in the flow tube experiments are much higher and lead to highly oxidized aerosols

ACPD
11, 7095–7112, 2011

(in the LV-OOA range, with an O:C up to ∼1). Taken together, the chamber and flow tube data map out the entire oxidation range of α-pinene SOA and span the whole range of O:C observed in ambient measurements. The oxidation of α-pinene also follows a slope of ∼ −0.5 in the Van Krevelen diagram, consistent with the observed evolution of SV-OOA to LV-OOA in ambient data. Also shown in Fig. 6 are individual compounds (with known H:C and O:C) that have been identified in α-pinene SOA (Jaoui and Kamens, 2001; Szmigielski et al., 2007), including both first-generation and higher generation oxidation products. On average, the composition change based on these identified products also follows a slope of ∼ −0.5, consistent with the change in bulk composition measured by the HR-AMS. For example, cis-pinonic acid ($C_{10}H_{16}O_3$) is a typical first-generation product, and its OH oxidation product, α,α-dimethyltricarballylic acid ($C_8H_{12}O_6$), is a tricarboxylic acid formed via fragmentation (Szmigielski et al., 2007). The oxidation of pinonic acid to α,α-dimethyltricarballylic acid also follows a line with a slope of ∼ −0.5. Furthermore, it can be seen from the molecular structures that while the cis-pinonic acid to α,α-dimethyltricarballylic acid transformation involves the loss of 2 carbons, there is a net gain of both OH and COOH functionalities (possibly through the loss of a carbonyl group to the C_2 fragment followed by the addition of two COOH groups) (Szmigielski et al., 2007), consistent with our hypotheses for the dominant chemical transformations in OOA aging. Further molecular-level studies of SOA aging are needed to elucidate the details within these trends.

3 Conclusions

By parameterizing organic aerosol H:C of SOA/OOA in terms of f_{43}, we are able to transform data in the triangle plot (f_{44} vs. f_{43}) into the Van Krevelen diagram (H:C vs. O:C). Ambient OOA components in the triangle plot map out a triangular space in Van Krevelen diagram, showing a range of H:C at lower oxidization; such variation decreases with increasing oxidation. Taking all the UMR and HR-AMS data together, it is found that on average, the change in the bulk composition of OOA as oxidation

ACPD
11, 7095–7112, 2011

progresses follows a line with a slope ∼ −0.5, which is shallower than the −1 slope proposed by Heald et al. (2010) and indicates that aging of OA is consistent with the addition of both COOH *and* OH functional groups without fragmentation, and/or the addition of COOH groups with C-C bond cleavage. This simplified view of bulk OOA aging can provide a useful guide for modeling the complex oxidation pathways and changes in OA chemical and physical properties with increased oxidation, and needs to be investigated in detail with molecular-level studies.

Supplementary material related to this article is available online at: http://www.atmos-chem-phys-discuss.net/11/7095/2011/acpd-11-7095-2011-supplement.pdf.

Acknowledgements. We thank grants from DOE (BER, ASR program) DEFG0208ER64627, NOAA NA08OAR4310565, and NSF ATM-0919189. We thank Paola Massoli for sharing the Boston College flow tube data and Jesse Kroll for helpful discussions.

References

Aiken, A. C., DeCarlo, P. F., and Jimenez, J. L.: Elemental Analysis of Organic Species with Electron Ionization High-Resolution Mass Spectrometry, Anal. Chem., 79, 8350–8358, doi:8310.1021/ac071150w, 2007.

Aiken, A. C., DeCarlo, P. F., Kroll, J. H., Worsnop, D. R., Huffman, J. A., Docherty, K. S., Ulbrich, I. M., Mohr, C., Kimmel, J. R., Sueper, D., Sun, Y., Zhang, Q., Trimborn, A., Northway, M., Ziemann, P. J., Canagaratna, M. R., Onasch, T. B., Alfarra, M. R., Prevot, A. S. H., Dommen, J., Duplissy, J., Metzger, A., Baltensperger, U., and Jimenez, J. L.: O/C and OM/OC ratios of primary, secondary, and ambient organic aerosols with high-resolution time-of-flight aerosol mass spectrometry, Environ. Sci. Technol., 42, 4478–4485, 2008.

Aiken, A. C., Salcedo, D., Cubison, M. J., Huffman, J. A., DeCarlo, P. F., Ulbrich, I. M., Docherty, K. S., Sueper, D., Kimmel, J. R., Worsnop, D. R., Trimborn, A., Northway, M., Stone, E. A., Schauer, J. J., Volkamer, R. M., Fortner, E., de Foy, B., Wang, J., Laskin, A., Shutthanandan, V., Zheng, J., Zhang, R., Gaffney, J., Marley, N. A., Paredes-Miranda, G., Arnott, W. P.,

ACPD
11, 7095–7112, 2011

Molina, L. T., Sosa, G., and Jimenez, J. L.: Mexico City aerosol analysis during MILAGRO using high resolution aerosol mass spectrometry at the urban supersite (T0) - Part 1: Fine particle composition and organic source apportionment, Atmos. Chem. Phys., 9, 6633–6653, doi:10.5194/acp-9-6633-2009, 2009.

Chhabra, P. S., Flagan, R. C., and Seinfeld, J. H.: Elemental analysis of chamber organic aerosol using an aerodyne high-resolution aerosol mass spectrometer, Atmos. Chem. Phys., 10, 4111–4131, doi:10.5194/acp-10-4111-2010, 2010.

Chhabra, P. S., Ng, N. L., Canagaratna, M. R., Corrigan, A. L., Russell, L. M., Worsnop, D. R., Flagan, R. C., and Seinfeld, J. H.: Elemental Composition and Oxidation of Chamber Organic Aerosol, in preparation, 2011.

DeCarlo, P. F., Ulbrich, I. M., Crounse, J., de Foy, B., Dunlea, E. J., Aiken, A. C., Knapp, D., Weinheimer, A. J., Campos, T., Wennberg, P. O., and Jimenez, J. L.: Investigation of the sources and processing of organic aerosol over the Central Mexican Plateau from aircraft measurements during MILAGRO, Atmos. Chem. Phys., 10, 5257–5280, doi:10.5194/acp-10-5257-2010, 2010.

Decesari, S., Mircea, M., Cavalli, F., Fuzzi, S., Moretti, F., Tagliavini, E., and Facchini, M. C.: Source attribution of water-soluble organic aerosol by nuclear magnetic resonance spectroscopy, Environ. Sci. Technol., 41, 2479–2484, 2007.

Docherty, K. S., Stone, E. A., Ulbrich, I. M., DeCarlo, P. F., Snyder, D. C., Schauer, J. J., Peltier, R. E., Weber, R. J., Murphy, S. M., Seinfeld, J. H., Grover, B. D., Eatough, D. J., and Jimenez, J. L.: Apportionment of Primary and Secondary Organic Aerosols in Southern California during the 2005 Study of Organic Aerosols in Riverside (SOAR-1), Environ. Sci. Technol., 42, 7655–7662, 2008.

Duplissy, J., DeCarlo, P. F., Dommen, J., Alfarra, M. R., Metzger, A., Barmpadimos, I., Prevot, A. S. H., Weingartner, E., Tritscher, T., Gysel, M., Aiken, A. C., Jimenez, J. L., Canagaratna, M. R., Worsnop, D. R., Collins, D. R., Tomlinson, J., and Baltensperger, U.: Relating hygroscopicity and composition of organic aerosol particulate matter, Atmos. Chem. Phys., 11, 1155–1165, doi:10.5194/acp-11-1155-2011, 2011.

Heald, C. L., Kroll, J. H., Jimenez, J. L., Docherty, K. S., DeCarlo, P. F., Aiken, A. C., Chen, Q., Martin, S. T., Farmer, D. K., and Artaxo, P.: A simplified description of the evolution of organic aerosol composition in the atmosphere, Geophys. Res. Lett., 37, L08803, doi:10.1029/2010GL042737, 2010.

Huang, X.-F., He, L.-Y., Hu, M., Canagaratna, M. R., Kroll, J. H., Ng, N. L., Zhang, Y.-H., Lin, Y.,

ACPD
11, 7095–7112, 2011

Xue, L., Sun, T.-L., Liu, X.-G., Shao, M., Jayne, J. T., and Worsnop, D. R.: Characterization of submicron aerosols at a rural site in Pearl River Delta of China using an Aerodyne High-Resolution Aerosol Mass Spectrometer, Atmos. Chem. Phys. Discuss., 10, 25841–25869, doi:10.5194/acpd-10-25841-2010, 2010a.

Huang, X.-F., He, L.-Y., Hu, M., Canagaratna, M. R., Sun, Y., Zhang, Q., Zhu, T., Xue, L., Zeng, L.-W., Liu, X.-G., Zhang, Y.-H., Jayne, J. T., Ng, N. L., and Worsnop, D. R.: Highly time-resolved chemical characterization of atmospheric submicron particles during 2008 Beijing Olympic Games using an Aerodyne High-Resolution Aerosol Mass Spectrometer, Atmos. Chem. Phys., 10, 8933–8945, doi:10.5194/acp-10-8933-2010, 2010b.

Jaoui, M. and Kamens, R. M.: Mass balance of gaseous and particulate products analysis from alpha-pinene/NO_x/air in the presence of natural sunlight, J. Geophys. Res.-Atmos., 106, 12541–12558, 2001.

Jimenez, J. L., Canagaratna, M. R., Donahue, N. M., Prevot, A. S. H., Zhang, Q., Kroll, J. H., DeCarlo, P. F., Allan, J. D., Coe, H., Ng, N. L., Aiken, A. C., Docherty, K. S., Ulbrich, I. M., Grieshop, A. P., Robinson, A. L., Duplissy, J., Smith, J. D., Wilson, K. R., Lanz, V. A., Hueglin, C., Sun, Y. L., Tian, J., Laaksonen, A., Raatikainen, T., Rautiainen, J., Vaattovaara, P., Ehn, M., Kulmala, M., Tomlinson, J. M., Collins, D. R., Cubison, M. J., Dunlea, E. J., Huffman, J. A., Onasch, T. B., Alfarra, M. R., Williams, P. I., Bower, K., Kondo, Y., Schneider, J., Drewnick, F., Borrmann, S., Weimer, S., Demerjian, K., Salcedo, D., Cottrell, L., Griffin, R., Takami, A., Miyoshi, T., Hatakeyama, S., Shimono, A., Sun, J. Y., Zhang, Y. M., Dzepina, K., Kimmel, J. R., Sueper, D., Jayne, J. T., Herndon, S. C., Trimborn, A. M., Williams, L. R., Wood, E. C., Middlebrook, A. M., Kolb, C. E., Baltensperger, U., and Worsnop, D. R.: Evolution of Organic Aerosols in the Atmosphere, Science, 326, 1525–1529, 2009.

Kroll, J. H., Smith, J. D., Che, D. L., Kessler, S. H., Worsnop, D. R., and Wilson, K. R.: Measurement of fragmentation and functionalization pathways in the heterogeneous oxidation of oxidized organic aerosol, Phys. Chem. Chem. Phys., 11, 8005–8014, 2009.

Kroll, J. H., Donahue, N. M., Jimenez, J. L., Kessler, S. H., Canagaratna, M. R., Wilson, K. R., Altieri, K. E., Mazzoleni, L. R., Wozniak, A. S., Bluhm, H., Mysak, E. R., Smith, J. D., Kolb, C. E., and Worsnop, D. R.: Carbon oxidation state as a metric for describing the chemistry of atmospheric organic aerosol, Nature Chemistry, 3, 133–139, doi:10.1038/nchem.948, 2011.

Massoli, P., Lambe, A. T., Ahern, A. T., Williams, L. R., Ehn, M., Mikkila, J., Canagaratna, M. R., Brune, W. H., Onasch, T. B., Jayne, J. T., Petaja, T., Kulmala, M., Laaksonen, A., Kolb, C. E., Davidovits, P., and Worsnop, D. R.: Relationship between aerosol oxidation level and

ACPD
11, 7095–7112, 2011

hygroscopic properties of laboratory generated secondary organic aerosol (SOA) particles, Geophys. Res. Lett., 37, L24801, doi:10.1029/2010GL045258, 2010.

Ng, N. L., Canagaratna, M. R., Zhang, Q., Jimenez, J. L., Tian, J., Ulbrich, I. M., Kroll, J. H., Docherty, K. S., Chhabra, P. S., Bahreini, R., Murphy, S. M., Seinfeld, J. H., Hildebrandt, L., Donahue, N. M., DeCarlo, P. F., Lanz, V. A., Prévôt, A. S. H., Dinar, E., Rudich, Y., and Worsnop, D. R.: Organic aerosol components observed in Northern Hemispheric datasets from Aerosol Mass Spectrometry, Atmos. Chem. Phys., 10, 4625–4641, doi:10.5194/acp-10-4625-2010, 2010.

Ng, N. L., Herndon, S. C., Trimborn, A., Canagaratna, M. R., Croteau, P., Onasch, T. M., Sueper, D., Worsnop, D. R., Zhang, Q., Sun, Y. L., and Jayne, J. T.: An Aerosol Chemical Speciation Monitor (ACSM) for routine monitoring of atmospheric aerosol composition, Aerosol Sci. Technol., in print, 2011.

Russell, L. M., Bahadur, R., and Ziemann, P. J.: Identifying organic aerosol sources by comparing functional group composition in chamber and atmospheric particles, Proc. Natl. Acad. Sci. USA, doi:10.1073/pnas.1006461108, 2011.

Sun, Y.-L., Zhang, Q., Schwab, J. J., Demerjian, K. L., Chen, W.-N., Bae, M.-S., Hung, H.-M., Hogrefe, O., Frank, B., Rattigan, O. V., and Lin, Y.-C.: Characterization of the sources and processes of organic and inorganic aerosols in New York city with a high-resolution time-of-flight aerosol mass apectrometer, Atmos. Chem. Phys., 11, 1581–1602, doi:10.5194/acp-11-1581-2011, 2011.

Szmigielski, R., Surratt, J. D., Gomez-Gonzalez, Y., Van der Veken, P., Kourtchev, I., Vermeylen, R., Blockhuys, F., Jaoui, M., Kleindienst, T. E., Lewandowski, M., Offenberg, J. H., Edney, E. O., Seinfeld, J. H., Maenhaut, W., and Claeys, M.: 3-methyl-1,2,3-butanetricarboxylic acid: An atmospheric tracer for terpene secondary organic aerosol, Geophys.Res. Lett., 34, L24811, doi:10.1029/2007GL031338, 2007.

Van Krevelen, D. W.: Graphical-statistical method for the study of structure and reaction processes of coal, Fuel, 24, 269–284, 1950.

Yu, J. Z., Cocker, D. R., Griffin, R. J., Flagan, R. C., and Seinfeld, J. H.: Gas-phase ozone oxidation of monoterpenes: Gaseous and particulate products, J. Atmos. Chem., 34, 207–258, 1999.

ACPD
11, 7095–7112, 2011

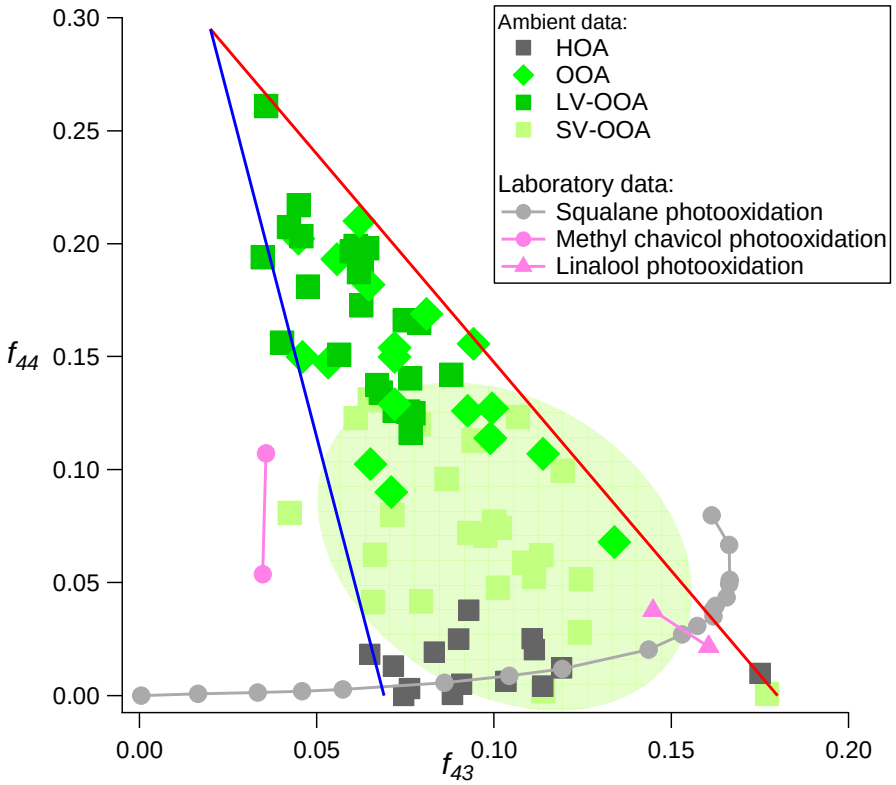

Fig. 1. Triangle plot (f_{44} vs. f_{43}) for all the OOA components from 43 ambient AMS datasets as well as selected laboratory data (adapted from Ng et al., 2010). The light green shaded area indicates the region where most of laboratory data fall into.

ACPD
11, 7095–7112, 2011

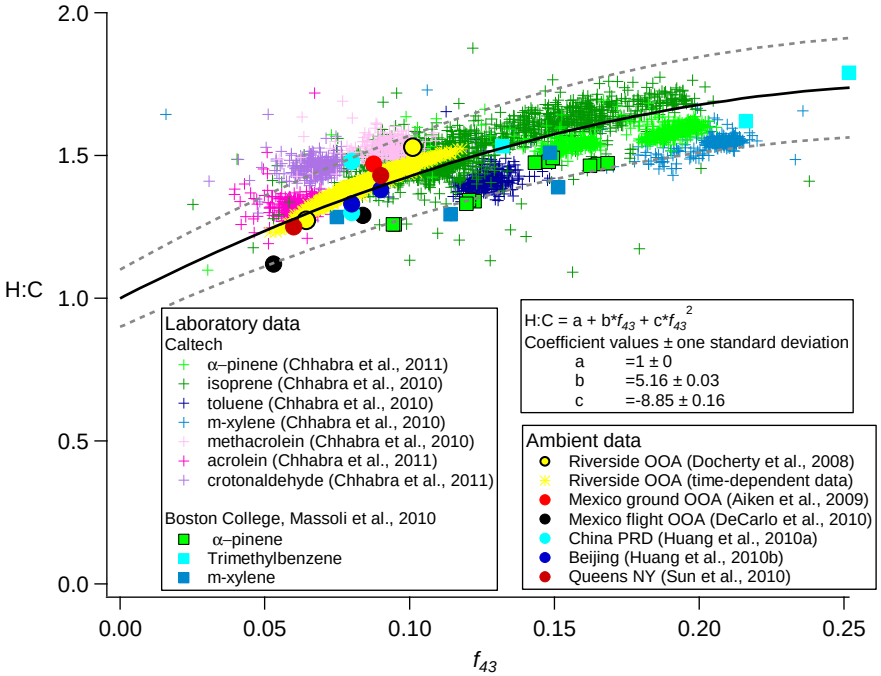

Fig. 2. Parameterization of H:C in terms of f_{43} for SOA/OOA, using OOA components obtained from PMF analysis of HR-AMS ambient datasets and SOA formed in laboratory studies. The dotted gray lines are ± 10% from the fitted line.

ACPD
11, 7095–7112, 2011

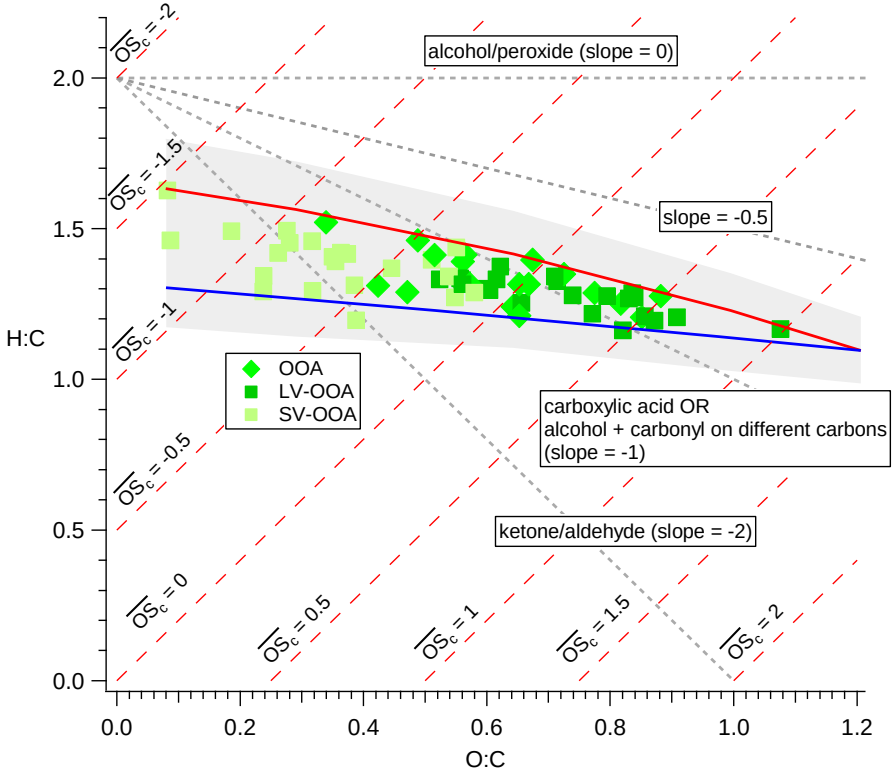

Fig. 3. Representation of all the OOA components into the VK-triangle diagram. The left and right sides of the triangle plot become the bottom and top lines in the Van Krevelen diagram, respectively. The light gray shaded region denotes the ± 10% uncertainty in the parameterization. The estimated carbon oxidation states ($\overline{OS}_C \approx 2$ O/C – H/C) are shown with the red dotted lines.

ACPD
11, 7095–7112, 2011

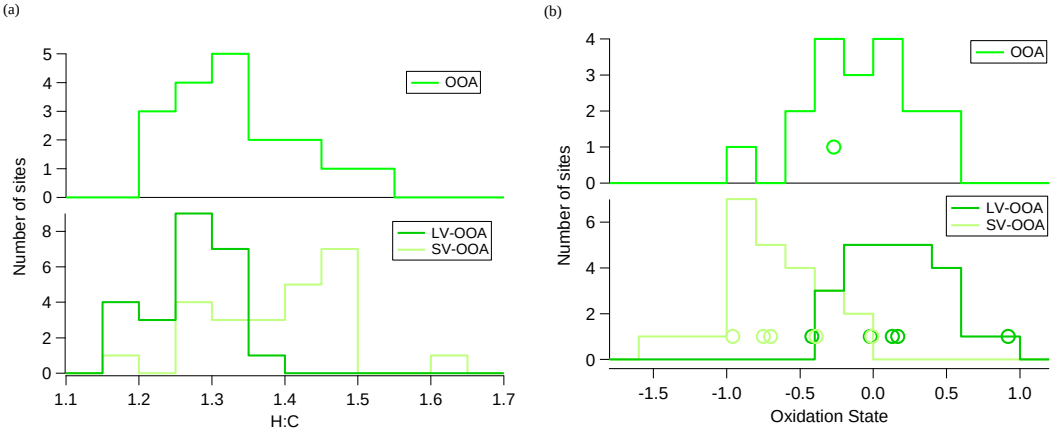

Fig. 4. **(a)** Histogram showing the distribution of the estimated H:C ratios observed across multiple sites. **(b)** Histogram showing the distribution of the estimated carbon oxidation states ($\overline{OS}_C \approx 2$ O/C – H/C) observed across multiple sites. The open circles are HR-AMS ambient data in which oxidation states are directly calculated from the data.

ACPD
11, 7095–7112, 2011

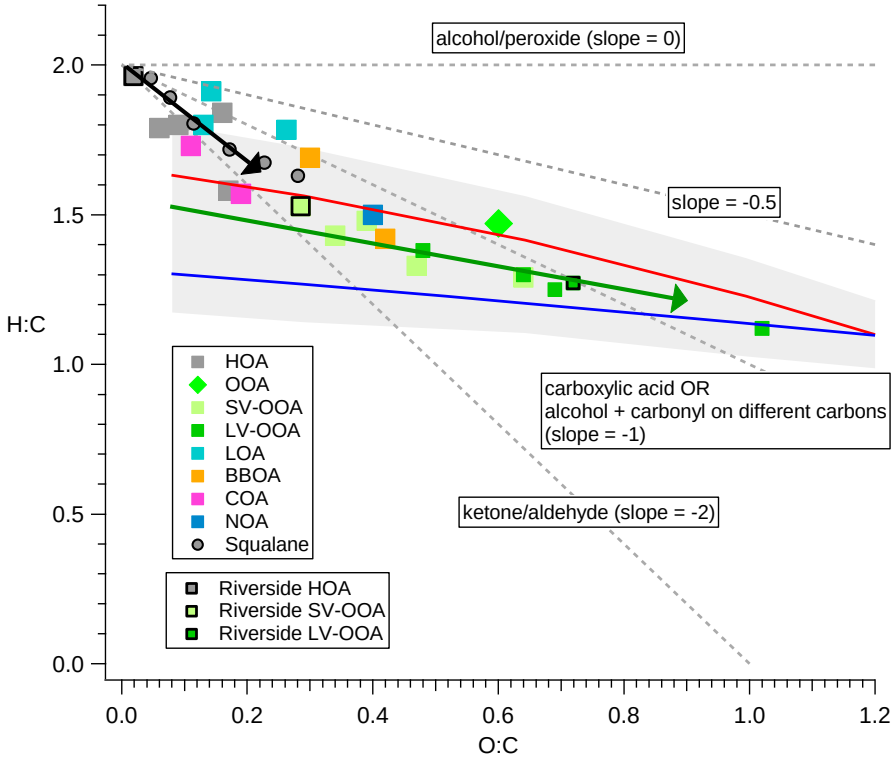

Fig. 5. VK-triangle diagram for the OA components from all sites with HR-AMS data and results from the heterogeneous oxidation of squalane. The light gray shaded region denotes the ± 10% uncertainty in the parameterization. (Note: LOA = local OA; BBOA = biomass burning OA; COA = cooking OA; NOA = nitrogen-enriched OA)

ACPD
11, 7095–7112, 2011

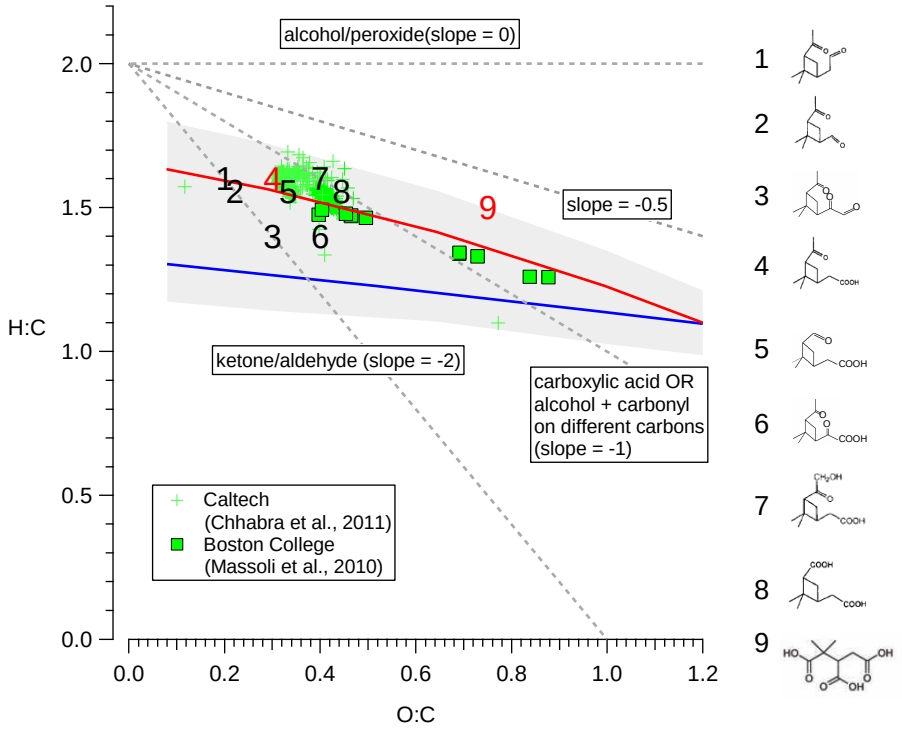

Fig. 6. VK-triangle diagram for α-pinene photooxidation, including HR-AMS data from both chamber and flow tube experiments. The light gray shaded region denotes the ± 10% uncertainty in the parameterization. The numbers correspond to individual molecular products in α-pinene SOA, with their structures being shown on the right. Product 4 is cis-pinonic acid and product 9 is α,α-dimethyltricarballylic acid.

ACPD
11, 7095–7112, 2011